Multi-channel Groupwise Registration to Construct an Ultrasound-Specific Fetal Brain Atlas

Ana I. L. Namburete[1(✉)], Raquel van Kampen[1], Aris T. Papageorghiou[2], and Bartłomiej W. Papież[1,3]

[1] Institute of Biomedical Engineering, Department of Engineering Science, University of Oxford, Oxford, UK
ana.namburete@eng.ox.ac.uk

[2] Nuffield Department of Obstetrics and Gynaecology, John Radcliffe Hospital, University of Oxford, Oxford, UK

[3] Big Data Institute, Li Ka Shing Centre for Health Information and Discovery, University of Oxford, Oxford, UK

Abstract. In this paper, we describe a method to construct a 3D atlas from fetal brain ultrasound (US) volumes. A multi-channel groupwise Demons registration is proposed to simultaneously register a set of images from a population to a common reference space, thereby representing the population average. Similar to the standard Demons formulation, our approach takes as input an intensity image, but with an additional channel which contains phase-based features extracted from the intensity channel. The proposed multi-channel atlas construction method is evaluated using a groupwise Dice overlap, and is shown to outperform standard (single-channel) groupwise diffeomorphic Demons registration. This method is then used to construct an atlas from US brain volumes collected from a population of 39 healthy fetal subjects at 23 gestational weeks. The resulting atlas manifests high structural overlap, and correspondence between the US-based and an age-matched fetal MRI-based atlas is observed.

1 Introduction

Tracking fetal growth and developmental progression is paramount in obstetric care. The fetal brain undergoes a predictable sequence of structural changes across gestation: from a smooth surface, to progressively bearing more folds [1]. This process follows a precise schedule, and delays are indicative of impaired brain maturation. Thus, the presence of a cerebral abnormality may be manifested by structural deviations from the norm. In order to detect such developmental deviations, an individual's image can be compared against an atlas that is representative of the healthy population. Atlases of the developing brain have been developed from magnetic resonance (MR) image data collected from infant and fetal subjects (reviewed in [2]). These atlases have provided a representation of brain anatomy in the womb, and have facilitated tissue segmentation, thereby

A. Melbourne and R. Licandro et al. (Eds.): DATRA/PIPPI 2018, LNCS 11076, pp. 76–86, 2018.
https://doi.org/10.1007/978-3-030-00807-9_8

enabling studies of structural growth and aiding the detection (or characterization) of fetal pathologies [2]. However, given that ultrasound (US) imaging forms one of the first steps in perinatal monitoring, there is still a need to create an *ultrasound-specific* atlas for use in routine care. This work presents a tool to automatically generate an atlas from 3D US images of the fetal brain.

The standard approach to construct an anatomical atlas is to perform one of state-of-the-art pairwise deformable registration algorithms [3] between the chosen (reference) volume and the remaining volumes from a data set. Such an approach is simple and easily scalable to large data sets, however it introduces a bias to registration results due to the selection of reference volume. That is, if the selected reference volume is an outlier then all registrations will estimate implausible transformations. Additionally, the transformation estimated using a pairwise approach accumulates inverse consistency and transitivity errors [4], which could be propagated to any subsequent analysis. Different approaches have been proposed to reduce transformation errors when building atlases, including statistical deformation models [5], linear [6] or geodesic [7,8] averaging of the transformations and intensity to produce the atlases. Approaches with simultaneous registration (i.e. *groupwise registration*) of all volumes in a dataset have been shown to reduce the bias introduced by selection of a fixed reference volume, and errors in the estimated displacement fields.

Developing intensity-based methods for registration of ultrasound images is challenging due to strong intensity inhomogeneities within tissues, and the presence of shadows, which cause partial, low-contrast boundaries. Local phase [9] and feature asymmetry (derived from the monogenic signal [10]) extract contrast-invariant structural information, and have been shown to improve analysis of US images in several tasks. Specifically, feature asymmetry (FA) has the potential to enhance tissue boundaries, and as such, has been extensively used to process fetal ultrasound data, where there are large structural changes (e.g. [11,12]). A hybrid intensity and local phase representation of US images has been applied to tumour tracking in 2D liver US [13], showing overall improved registration accuracy. Realizing the potential of FA to enhance and sharpen the sonographic landmarks necessary for accurate registration, this work explores its inclusion as additional image channels for US atlas construction.

In this paper, we present a framework to construct the first 3D atlas of the fetal brain using non-rigid groupwise registration of US images. Our framework extends a standard groupwise registration [4] to its multi-channel counterpart using a composite image representation to improve the registration of tissue interfaces in US data. The proposed multi-channel image representation comprises of ultrasound intensities and features extracted using different FA scales, thereby representing boundaries of different sizes in a multiscale manner. The presented evaluation shows that the presented method is capable of constructing an atlas from fetal brain US data, and at the same time, the performed quantitative analysis shows that our method outperforms standard intensity-based, and single channel image registration methods.

2 Materials and Methods

2.1 Fetal Dataset and Preprocessing

The fetal US images used in this work comprised of 39 volumes ($247 \times 190 \times 179$ voxels) with known age of 23 gestational weeks (GW). The sonographic volumes of the fetal head were obtained from the INTERGROWTH-21st study database [14], which were collected using a Philips HD9 curvilinear probe at a 2–5 MHz wave frequency. After alignment [15], all volumes were resampled to an isotropic voxel size ($0.6 \times 0.6 \times 0.6$ mm) and resized to $160 \times 160 \times 160$ voxels.

2.2 Atlas Construction

Given a set of M images, the goal of atlas construction is to find a set of transformations $\mathcal{T}$, each of which maps its corresponding image $\mathbf{I}_m$ to a common reference space: $\mathcal{T} : \{\boldsymbol{T}_{mR} : \mathbf{I}_m \mapsto \mathbf{I}_R, m = 1, \ldots, M\}$. This typically comprises of two steps: a global transformation to correct for size and growth differences, followed by a non-rigid registration to account for local morphological differences.

Sonographic scans of the fetal head were first rigidly aligned using the method proposed in [15]. Briefly, a slice-wise classifier segmented the skull boundaries and predicted the relative position of the slice in the brain volume. This information was then combined to estimate a similarity transformation modelling 9 degrees of freedom (namely, rotation, translation, and isotropic scaling) to linearly register all volumes to a standard (atlas) space. One of the challenges of processing fetal brain US is that the ultrasound signal is attenuated by the cranial bones in its path, and the concave shape also refracts it and creates reverberation artifacts. This affects the visibility of anatomical boundaries, particularly in the cerebral hemisphere proximal to the US probe. Since only one of the hemispheres has clearly visible structures, this hemisphere is mirrored across the midsagittal plane. This generates a *complete* representation of the brain, thereby making an assumption of brain symmetry, for simplicity [16].

The non-rigid image registration used in this work, is built on the groupwise deformable registration proposed in [4,17]. The implicit reference groupwise registration reduces bias introduced by selection of a reference volume by jointly estimating the transformation between all volumes in the dataset to an *unknown* reference volume. This process is defined as the following optimization problem:

$$\arg\min_{\boldsymbol{u}} \left(\sum_{m}^{M} \sum_{n,n\neq m}^{M} \int_{\Omega} Sim\left(\mathbf{I}_m(\boldsymbol{T}_{mR}(\boldsymbol{x})), \mathbf{I}_n(\boldsymbol{T}_{nR}(\boldsymbol{x}))\right) d\boldsymbol{x} + \right. \tag{1}$$

$$\left. \alpha \sum_{m}^{M} \int_{\Omega} Reg(\boldsymbol{u}_{mR}(\boldsymbol{x})) d\boldsymbol{x} \right) \tag{2}$$

where Sim and Reg denote the similarity measure and regularisation term, respectively, α is the weighting parameter, $\boldsymbol{T}_{mR} = \boldsymbol{x} + \boldsymbol{u}_{mR}(\boldsymbol{x})$ (or $\boldsymbol{T}_{nR} =$

$\boldsymbol{x} + \boldsymbol{u}_{nR}(\boldsymbol{x})$) is the transformation from volume $\mathbf{I}_m$ (or $\mathbf{I}_n$) to the implicit reference volume $\mathbf{I}_R$ at spatial position $\boldsymbol{x}$. The $\boldsymbol{u}_{mR}$ (or $\boldsymbol{u}_{nR}$) represents a subsequent displacement field, Ω is the volume domain, and M is the number of volumes to be registered. The *implicit* reference volume is iteratively updated based on all the volumes deformed during the displacement field estimation process. In this work, we choose the diffeomorphic Demons framework [18], where optimisation iteratively alternates between minimising the energy related to the similarity measure Sim and the regularization term Reg performed via Gaussian smoothing of the estimated displacement fields. In order to establish anatomically meaningful correspondences between brain US volumes, we replace state-of-the-art intensity differences used in the classic Demons by a multi-channel feature-based representation of the US volumes. The implementation details for efficient Demons-like implicit reference groupwise registration can be found in [19].

2.3 Feature Extraction

The monogenic signal uses the Riesz transform to generate a representation of an image in the frequency domain [20]. By applying an appropriately selected bandpass filter ($f_{\{o,e\}}$), the signal can be decomposed into local structural (phase and orientation) and energetic (amplitude) information. The phase component extracts contrast-invariant, structural information, which is particularly useful in recovering feature asymmetry (FA) [21]. FA is a measure of the extent to which a structure around an image voxel is locally *asymmetric*, thus representing a step-edge [10,21]. The FA edge image $\hat{\mathbf{I}}$ of an input image $\mathbf{I}$ is recovered as:

$$\hat{\mathbf{I}} = \frac{\lfloor |f_{o,\lambda}(\mathbf{I})| - |f_{e,\lambda}(\mathbf{I})| - t \rfloor}{\sqrt{f_{o,\lambda}(\mathbf{I})^2 + f_{e,\lambda}(\mathbf{I})^2 + \varepsilon}} \tag{3}$$

where λ represents the filter scale, f_o and f_e represent the odd and even parts of the signal, t is a threshold that controls the sensitivity of the response, $\lfloor \cdot \rfloor$ sets negative values to zero, and ε is a filter regularization parameter which prevents division by zero.

FA allows edge features to be obtained at different centre-wavelengths, λ. The centre frequency is equivalent to the scale of the bandpass filter $f_{\{o,e\},\lambda}$ (i.e. size of structures of interest) used to the calculate the monogenic signal. In fetal brain US images, the anatomical boundaries appear as step-edges and ridge-like structures, which are best extracted with a log-Gabor filter [11]. Given an US image, $\mathbf{I}$, a corresponding FA edge image $\hat{\mathbf{I}}$ is defined to highlight structural boundaries [10,21]. An FA image typically detects thick edges which are thinned by applying non-maximum suppression for improved boundary localization. Here, we explore the effect of supplementary structural information for atlas construction by varying the centre frequency at which the monogenic signal was recovered from the images, $\lambda = [0.025, 0.425]$ (Fig. 1). The other parameters were empirically set to $t = 0.5$ and $\varepsilon = 10^{-6}$.

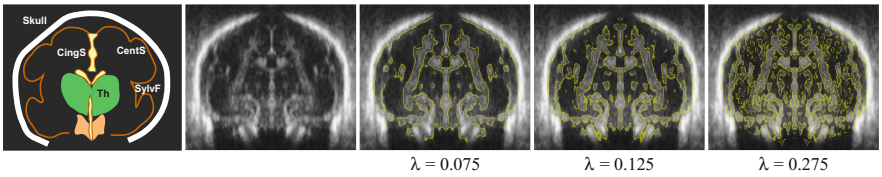

Fig. 1. Schematic of a coronal view of the fetal brain at 23 GW, and a typical US scan. Feature asymmetry edge images are shown at varying centre-frequency wavelengths, $\lambda = \{0.075, 0.125, 0.275\}$, overlaid in yellow. (Color figure online)

2.4 Evaluation Metrics

Ten brain volumes were linearly registered using [15] and anatomical regions were manually segmented and verified by an expert with 10 years' experience and a senior sonographer. The segmented regions of interest ($\mathbf{V}^k$) included the brain stem (BS), cavum septum pellucidum (CSP), thalamus (TH), and white matter (WM) (Fig. 2c). In order to evaluate registration performance, we compute the average relative overlap (ARO) for each of the $K = 4$ regions as follows [4]:

$$ARO = \frac{1}{N(N-1)} \sum_{\substack{j=1,\\ j \neq i}}^{N} \sum_{i=1}^{N} \frac{\sum_K \mathbf{V}_i^k \cap \mathbf{V}_j^k}{\sum_K \mathbf{V}_i^k \cup \mathbf{V}_j^k} \tag{4}$$

where $\mathbf{V}_i^k = \mathbf{V}_i^k\left(\mathcal{T}_{iR}(\mathbf{I})\right)$, K is the number structures, and N is the number of annotated volumes.

All experiments were performed on an Intel i7 2.80 GHz quad-core machine (32 GB RAM) with a C++ implementation of the diffeomorphic Demons algorithm.

3 Results and Discussion

3.1 Registration of Anatomical Structures

In the first experiment, we explored different formulations of the groupwise registration algorithm to construct an atlas that maximizes anatomical correspondence between the neurosonographic images. By varying the diffusion parameter of the Demons-like forces ($\sigma_d = [0.25, 5.0]$), we find that the best performance is achieved with $\sigma_d = 1.0$ (ARO > 0.868 for WM, Fig. 2a), and gradually decreases as σ_d increases. This behaviour was observed regardless of input: single- or multi-channel.

Furthermore, we explored the effect of FA wavelength (scale) selection by varying λ from 0.025 to 0.425. Figure 2b shows the ARO averaged across all four structures. The groupwise approach outperformed the linearly aligned data, regardless of input. However, the multi-channel Demons (intensity + sFA) outperformed single-channel Demons (intensity) only for scales $\lambda = \{0.075, 0.125, 0.175\}$.

For further comparison, we explored the performance of a multi-channel Demons with multi-scale feature extraction by combining the features from the best FA scales ($\lambda = 0.075, 0.125, 0.175$) into the second input channel. This yielded the highest structural overlap (ARO $= 0.8029 \pm 0.049$) and was selected as the best method for atlas construction.

Figure 2c shows the result of applying the groupwise registration to the set of ten volumes for which corresponding segmentations were available. The atlases were constructed by averaging the images after affine registration, and then further transformed by the groupwise registration. There is high consensus between the structures, as observed in the probability maps, which is corroborated by the groupwise ARO of the resulting atlas (Table 1).

To further examine the anatomical agreement recovered by the groupwise registration algorithm, we compared the average segmentation maps obtained by transforming the annotated images, with a segmentation of the resulting groupwise atlas. High volumetric overlap was also observed for all four structures (mean ARO $= 0.8580 \pm 0.036$).

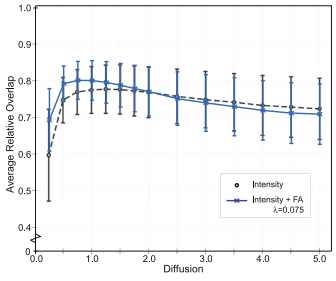

(a)

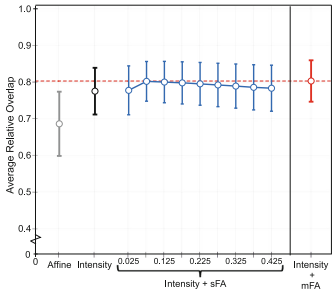

(b)

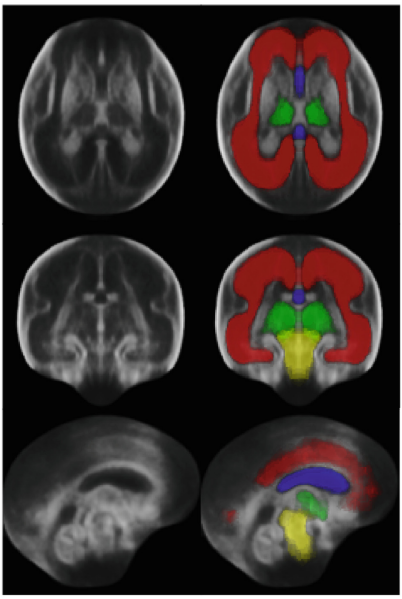

(c)

Fig. 2. (a) Registration regularization parameter (σ_d) versus average relative overlap (ARO). (b) Different atlas construction methods plotted against ARO. (c) Resulting US atlas constructed using intensity and multi-scale FA from $n = 10$ volumes for which segmentations were available. Denser colour signifies higher overlap.

3.2 Construction of Population Brain Atlas

In the second experiment, we applied the proposed multi-channel groupwise registration algorithm to 39 brain volumes to construct an atlas. Figure 3 shows atlases constructed by averaging the images after the affine registration [15], and after non-rigid registration with either a single (intensity) channel, or multiple channels (i.e. intensity and feature asymmetry). It is evident that the atlases constructed with groupwise registration had higher anatomical definition, and more distinct boundaries. Structural clarity was even higher in the atlas constructed with multi-channel inputs.

In order to visualize the structural variation within the healthy fetal cohort at 23 GW, we performed principal component analysis (PCA) of the deformation fields estimated from the 39 volumes. Figure 5 demonstrates the first four

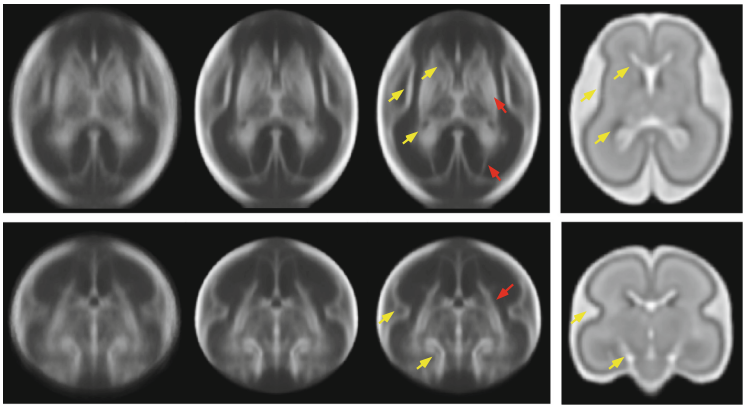

Fig. 3. Visual comparison between fetal brain atlases constructed from $n = 39$ US volumes at 23 GW using affine (first column), intensity-based (second column), and multi-channel groupwise methods (third column). Comparison to MRI-based fetal atlas at 23 GW shows the presence of similar structures in both modalities [22] (yellow arrows), but some structures are better observed in US images (red arrows). (Color figure online)

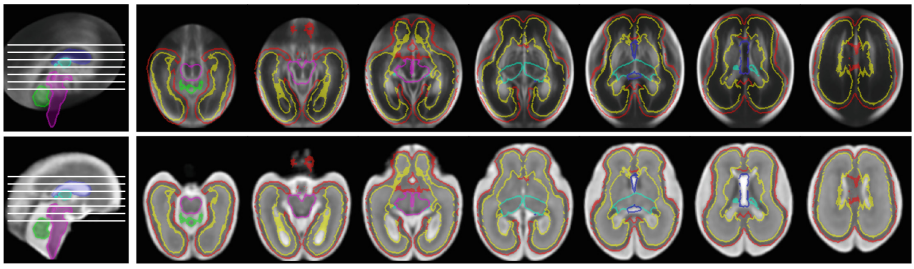

Fig. 4. Volumetric US atlas with superimposed segmentation of four structures from a fetal MR atlas at 23 GW (obtained from Gholipour et al. [22]).

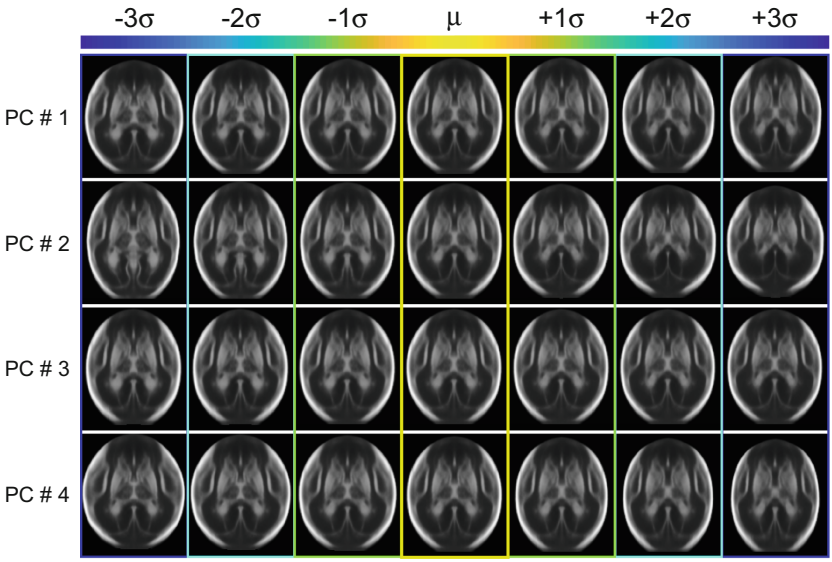

Fig. 5. Principal component analysis (PCA) result display the mean brain ±3 standard deviations (i.e. $\mu \pm 3\sigma$) for the first four components. All modes show realistic representations of the brain.

components, altogether explaining 65.6% of the variation at this gestational age. PC1, PC2, and PC4 display variations in anatomical shape and global eccentricity of the brain. Small changes in ventricular shape are particularly observed around the posterior lateral ventricles and the cortical plate in PC1. Nonetheless, all modes of variation demonstrate realistic representations of the brain at 23 GW.

3.3 Comparison to Existing Fetal Atlas

In order to assess the quality of the resulting atlas, Fig. 4 compares our US-specific atlas with a MRI-based fetal template at 23 GW generated by Gholipour et al. [22]. The contours of the latter are superimposed on the US-based atlas constructed from $n = 39$ volumes. Here, we can visually determine that despite there not being a direct intensity mapping between the two, there is a good match between the shape and location of the structures in both modalities at this gestational week. This illustrates the complementarity between the modalities, and presents opportunities to transfer anatomical insights from one to the other, and the possibility to facilitate analysis of fetal brain US with information contained within MRI models of development (e.g. [22]). The fact that structures such as the basal ganglia are better visible in the US-based atlas (Fig. 3) also presents new opportunities for use of neurosonographic data to study structural development.

Table 1. Average relative overlap for all four structures on 10 annotated volumes. Intensity: single-channel Demons. Intensity+sFA: multi-channel, single-scale demons ($\lambda = 0.075$). Intensity+mFA: multi-channel, multi-scale Demons with FA scales $\lambda = \{0.075, 0.125, 0.175\}$.

Method	Structural ARO ($\bar{D}^k$)				Mean ARO
	WM	TH	CSP	BS	
Linear only [15]	0.8174	0.6467	0.6379	0.6412	0.6858 ± 0.076
Intensity	0.8680	0.7383	0.7289	0.7652	0.7751 ± 0.055
Intensity + sFA	0.8829	0.7672	0.7806	**0.7771**	0.8019 ± 0.047
Intensity + mFA	**0.8873**	**0.7680**	**0.7824**	0.7738	$\mathbf{0.8029 \pm 0.049}$
Structural volume (cm^3)	37.64	1.954	0.449	1.233	–

4 Conclusion

In this paper, we present the first fetal brain atlas constructed from US data. The proposed multi-channel Demons formulation takes as input an image with intensity and feature-enhanced channels. It was shown to outperform a single-channel Demons registration approach, generating high structural overlap in the resulting atlas. Comparison with an age-matched MR atlas demonstrated similarities in the shape and presence of key anatomies in both imaging modalities, but also revealed new structures that are better observed in the US atlas. Given the formulation of the proposed method, it is expected that it should extend to a broader gestational age range.

Acknowledgements. A. Namburete is grateful for support from the Royal Academy of Engineering under the Engineering for Development Research Fellowship scheme. B. Papiez acknowledges Oxford NIHR Biomedical Research Centre (Rutherford Fund Fellowship at HDR UK). We thank the INTERGROWTH-21st and INTERBIO-21st Consortia for provision of 3D fetal US image data.

References

1. Toi, A., Lister, W.S., Fong, K.W.: How early are fetal cerebral sulci visible at prenatal ultrasound and what is the normal pattern of early fetal sulcal development? Ultrasound Obstet. Gynecol. **24**(7), 706–715 (2004)
2. Makropoulos, A., Counsell, S.J., Rueckert, D.: A review on automatic fetal and neonatal brain MRI segmentation. NeuroImage **170**, 231–248 (2018)
3. Sotiras, A., Davatzikos, C., Paragios, N.: Deformable medical image registration: a survey. IEEE Trans. Med. Imaging **32**(7), 1153–1190 (2013)
4. Geng, X., Christensen, G.E., Gu, H., Ross, T.J., Yang, Y.: Implicit reference-based group-wise image registration and its application to structural and functional MRI. NeuroImage **47**(4), 1341–1351 (2009)
5. Rueckert, D., Frangi, A.F., Schnabel, J.A.: Automatic construction of 3-D statistical deformation models of the brain using nonrigid registration. IEEE Trans. Med. Imaging **22**(8), 1014–1025 (2003)

6. Guimond, A., Meunier, J., Thirion, J.: Average brain models: a convergence study. Comput. Vis. Image Underst. **77**(2), 192–210 (2000)
7. Avants, B., Gee, J.C.: Geodesic estimation for large deformation anatomical shape averaging and interpolation. Neuroimage **23**, S139–S150 (2004)
8. Joshi, S., Davis, B., Jomier, M., Gerig, G.: Unbiased diffeomorphic atlas construction for computational anatomy. NeuroImage **23**, S151–S160 (2004)
9. Mellor, M., Brady, M.: Non-rigid multimodal image registration using local phase. In: Barillot, C., Haynor, D.R., Hellier, P. (eds.) MICCAI 2004. LNCS, vol. 3216, pp. 789–796. Springer, Heidelberg (2004). https://doi.org/10.1007/978-3-540-30135-6_96
10. Bridge, C.P.: Introduction to the monogenic signal. CoRR abs/1703.09199 (2017)
11. Namburete, A.I.L., Stebbing, R.V., Kemp, B., Yaqub, M., Papageorghiou, A.T., Alison Noble, J.: Learning-based prediction of gestational age from ultrasound images of the fetal brain. Med. Image Anal. **21**(1), 72–86 (2015)
12. Rueda, S., Knight, C.L., Papageorghiou, A.T., Noble, J.A.: Feature-based fuzzy connectedness segmentation of ultrasound images with an object completion step. Med. Image Anal. **26**(1), 30–46 (2015)
13. Cifor, A., Risser, L., Chung, D., Anderson, E.M., Schnabel, J.A.: Hybrid feature-based diffeomorphic registration for tumor tracking in 2-D liver ultrasound images. IEEE Trans. Med. Imaging **32**(9), 1647–1656 (2013)
14. Papageorghiou, A.T., et al.: International Fetal and Newborn Growth Consortium for the 21st Century (INTERGROWTH-21st): International standards for fetal growth based on serial ultrasound measurements: the Fetal Growth Longitudinal Study of the INTERGROWTH-21st Project. Lancet **384**(9946), 869–79 (2014)
15. Namburete, A.I., Xie, W., Yaqub, M., Zisserman, A., Noble, J.A.: Fully-automated alignment of 3D fetal brain ultrasound to a canonical reference space using multi-task learning. Med. Image Anal. **46**, 1–14 (2018)
16. Namburete, A.I.L., Xie, W., Noble, J.A.: Robust regression of brain maturation from 3D fetal neurosonography using CRNs. In: Cardoso, M.J., et al. (eds.) FIFI/OMIA -2017. LNCS, vol. 10554, pp. 73–80. Springer, Cham (2017). https://doi.org/10.1007/978-3-319-67561-9_8
17. Papiez, B.W., Matuszewski, B.J., Shark, L.K., Quan, W.: Facial expression recognition using diffeomorphic image registration framework. In: Latorre Carmona P., Sánchez J., Fred A. (eds.) Mathematical Methodologies in Pattern Recognition and Machine Learning. Springer Proceedings in Mathematics & Statistics, vol. 30. Springer, New York (2013). https://doi.org/10.1007/978-1-4614-5076-4_12
18. Vercauteren, T., Pennec, X., Perchant, A., Ayache, N.: Symmetric log-domain diffeomorphic registration: a demons-based approach. In: Metaxas, D., Axel, L., Fichtinger, G., Székely, G. (eds.) MICCAI 2008. LNCS, vol. 5241, pp. 754–761. Springer, Heidelberg (2008). https://doi.org/10.1007/978-3-540-85988-8_90
19. Papież, B.W., McGowan, D.R., Skwarski, M., Higgins, G.S., Schnabel, J.A., Brady, M.: Fast groupwise 4D deformable image registration for irregular breathing motion estimation. In: Klein, S., Staring, M., Durrleman, S., Sommer, S. (eds.) WBIR 2018. LNCS, vol. 10883, pp. 37–46. Springer, Cham (2018). https://doi.org/10.1007/978-3-319-92258-4_4
20. Felsberg, M., Sommer, G.: The monogenic signal. IEEE Trans. Sig. Process. **49**(12), 3136–3144 (2001)

21. Kovesi, P.: Invariant Measures of Image Features from Phase Information. Ph.D thesis, The University of Western Australia (1996)
22. Gholipour, A., et al.: A normative spatiotemporal MRI atlas of the fetal brain for automatic segmentation and analysis of early brain growth. Sci. Rep. **7**(1), 1 (2017)